AD-A040 100 RENSSELAER POLYTECHNIC INST TROY N Y DEPT OF MECHANI--ETC F/G 20/14
A PERTURBATION ANALYSIS OF THE ATTENUATION AND DISPERSION OF SU--ETC(U)
APR 77 H F TIERSTEN, B K SINHA N00014-76-C-0368
UNCLASSIFIED TR-21 NL

1 OF 1
ADA040 100

END

DATE FILMED
6-77

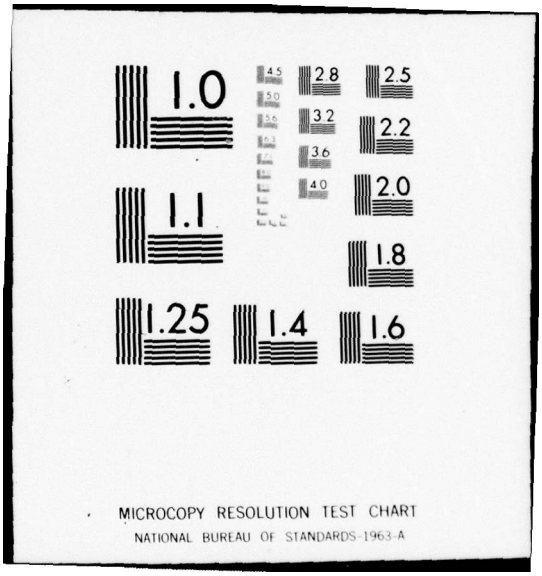
1.0
1.1
1.25
1.4
1.6
1.8
2.0
2.2
2.5
2.8
3.2
3.6
4.0
4.5
5.0
5.6
MICROCOPY RESOLUTION TEST CHART
NATIONAL BUREAU OF STANDARDS-1963-A

Rensselaer Polytechnic Institute
Troy, New York 12181

A PERTURBATION ANALYSIS OF THE ATTENUATION AND DISPERSION OF SURFACE WAVES

by

H.F. Tiersten and B.K. Sinha

Office of Naval Research
Contract N00014-76-C-0368
Project NR 318-009
Technical Report No. 21

April 1977

Rensselaer Polytechnic Institute

Troy, New York 12181

A PERTURBATION ANALYSIS OF THE ATTENUATION AND DISPERSION OF SURFACE WAVES

by

H.F. Tiersten and B.K. Sinha

Office of Naval Research
Contract N00014-76-C-0368
Project NR 318-009
Technical Report No. 21

April 1977

Unclassified

SECURITY CLASSIFICATION OF THIS PAGE (When Data Entered)

REPORT DOCUMENTATION PAGE

READ INSTRUCTIONS BEFORE COMPLETING FORM

1. REPORT NUMBER: TR [redacted] 21	2. GOVT ACCESSION NO.
3. RECIPIENT'S CATALOG NUMBER	
4. TITLE (and Subtitle): A Perturbation Analysis of the Attenuation and Dispersion of Surface Waves	5. TYPE OF REPORT & PERIOD COVERED: Technical rept.
6. PERFORMING ORG. REPORT NUMBER	
7. AUTHOR(s): H.F. Tiersten and B.K. Sinha	8. CONTRACT OR GRANT NUMBER(s): N00014-76-C-0368
9. PERFORMING ORGANIZATION NAME AND ADDRESS: Rensselaer Polytechnic Institute, Troy, New York 12181	10. PROGRAM ELEMENT, PROJECT, TASK AREA & WORK UNIT NUMBERS: NR 318-009
11. CONTROLLING OFFICE NAME AND ADDRESS: Office of Naval Research, Physics Branch, Washington, D.C.	12. REPORT DATE: April [redacted]977
	13. NUMBER OF PAGES: 31
14. MONITORING AGENCY NAME & ADDRESS (if different from Controlling Office)	15. SECURITY CLASS. (of this report): Unclassified
	15a. DECLASSIFICATION/DOWNGRADING SCHEDULE

16. DISTRIBUTION STATEMENT (of this Report)

Distribution of this document is unlimited

17. DISTRIBUTION STATEMENT (of the abstract entered in Block 20, if different from Report)

18. SUPPLEMENTARY NOTES

19. KEY WORDS (Continue on reverse side if necessary and identify by block number)

Surface waves	Attenuation	Electrical conductivity
Piezoelectricity	Dispersion	Thin films
Elasticity	Air loading	Sheet conductivity
Perturbations	Fluid viscosity	Iteration procedure

20. ABSTRACT (Continue on reverse side if necessary and identify by block number)

A perturbation formulation of the equations of linear piezoelectricity is obtained using a Green's function approach. Although the resulting equation for the first perturbation of the eigenvalue strictly holds for real perturbations of real eigenvalues only, it is formally extended to the case of purely imaginary perturbations of real eigenvalues. The extended equation is applied in the calculation of the attenuation of surface waves due to the finite electrical conductivity of thin metal films plated on the surface and air loading.

next page

DD FORM 1 JAN 73 1473 EDITION OF 1 NOV 65 IS OBSOLETE S/N 0102-014-6601

Unclassified

SECURITY CLASSIFICATION OF THIS PAGE (When Data Entered)

The influence of the viscosity of the air is included in the air loading analysis, and the calculated attenuation increases accordingly. Since the metal films are thin compared with a wavelength, an approximate thin plate conductivity equation is employed in the determination of the attenuation due to the electrical conductivity of the films. The resulting attenuation is obtained over a very large range of values of sheet conductivity. This is accomplished by using the equation for the first perturbation of the eigenvalue iteratively to determine the solution and attendant attenuation to any desired degree of accuracy. The phase velocity dispersion curve due to the mechanical effect of a thin film plated on a substrate is determined for relatively large wavelengths by employing the perturbation equation iteratively, and excellent agreement is obtained with the results of other more direct approaches. The calculations have been performed for an aluminum film on either ST-cut quartz or Y-Z lithium niobate.

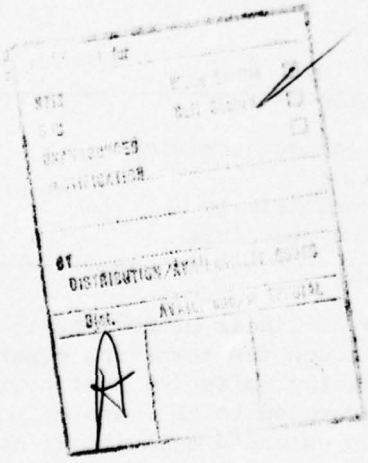

A PERTURBATION ANALYSIS OF THE ATTENUATION AND DISPERSION OF SURFACE WAVES

H.F. Tiersten and B.K. Sinha
Department of Mechanical Engineering,
Aeronautical Engineering & Mechanics
Rensselaer Polytechnic Institute
Troy, New York 12181

ABSTRACT

A perturbation formulation of the equations of linear piezoelectricity is obtained using a Green's function approach. Although the resulting equation for the first perturbation of the eigenvalue strictly holds for real perturbations of real eigenvalues only, it is formally extended to the case of purely imaginary perturbations of real eigenvalues. The extended equation is applied in the calculation of the attenuation of surface waves due to the finite electrical conductivity of thin metal films plated on the surface and air loading. The influence of the viscosity of the air is included in the air loading analysis, and the calculated attenuation increases accordingly. Since the metal films are thin compared with a wavelength, an approximate thin plate conductivity equation is employed in the determination of the attenuation due to the electrical conductivity of the films. The resulting attenuation is obtained over a very large range of values of sheet conductivity. This is accomplished by using the equation for the first perturbation of the eigenvalue iteratively to determine the solution and attendant attenuation to any desired degree of accuracy. The phase velocity dispersion curve due to the mechanical effect of a thin film plated on a substrate is determined for relatively large wavelengths by employing the perturbation equation iteratively, and excellent agreement is obtained with the results of other more direct approaches. The calculations have been performed for an aluminum film on either ST-cut quartz or Y-Z lithium niobate.

1. Introduction

The attenuation of acoustic surface waves propagating along electroded piezoelectric substrates arises from a number of different causes. In a manner of speaking, these can be loosely categorized as substrate and electrode material attenuation and air loading. The material attenuation is a result of material viscosity and electrical and thermal conductivity. In the substrate the viscosity is most important, the thermal conductivity of secondary importance and the electrical conductivity is negligible. In the thin metal film the electrical conductivity is of primary importance and the viscosity and thermal conductivity are of secondary importance. In any event in this work the attenuation due to the finite electrical conductivity of the thin electrode plating and air loading are determined. Measurements of attenuation due to a number of the aforementioned causes have been made[1-5].

The attenuation of surface waves due to air loading was first treated analytically by Campbell and Jones[6], who ignored the influence of the viscosity of the air and, consequently, obtained values of attenuation below those measured by Slobodnik[5]. Subsequently, Auld[7] obtained results identical with those of Ref.6 using his first order piezoelectric perturbation theory. The attenuation of acoustic surface waves due to an adjacent semiconducting film has been calculated by Ingebrigtsen[8] by means of a perturbation procedure.

In this paper a piezoelectric perturbation theory is obtained from a Green's function formulation[9] of the equations of linear piezoelectricity[10]. The resulting equation for the first perturbation of the eigenvalue is applied in the determination of the attenuation of surface waves due to the finite electrical conductivity of thin metal films plated on the surface and air loading. The directly determined time attenuation is converted to spatial attenuation. The resulting perturbation expression for the spatial attenuation is

similar to that of Auld[7]. In the case of attenuation due to air loading the stress in the air due to the unperturbed surface wave displacement field is inserted in the equation for the first perturbation of the eigenvalue. The influence of viscosity is included in addition to fluid pressure in the analysis of the air. As a consequence the calculated attenuation due to air loading is larger than that of either Ref.6 or 7 and is in excellent agreement with the measurements of Szabo and Slobodnik[11] for ST-cut quartz and Slobodnik[5] for lithium niobate.

Since the aforementioned metal films are thin compared with a wavelength, an approximate thin plate conductivity equation[12] is obtained, which enables the entire electrical conductivity effect of the plating to be treated as a boundary condition at the surface of the substrate. This approximate thin plate conductivity equation, but with a sign difference, has been employed by Adler[13] in a treatment of semiconducting thin films. The attenuation resulting from the conductivity of the thin film is determined by employing the aforementioned thin plate conductivity equation in the equation for the first perturbation of the eigenvalue in the usual manner. However, in this attenuation analysis the perturbation equation is used successively to increment the solution at one value of sheet conductivity from the previous solution at a nearby value of sheet conductivity, because we are interested in the attenuation over a large range of values of sheet conductivity. In addition, the perturbation equation is used iteratively at a fixed value of sheet conductivity to determine the solution and attendant attenuation to any desired degree of accuracy. With this latter procedure small changes in the phase velocity are obtained as well as the attenuation. However, we find that in this manner we are unable to obtain the attenuation over an impractical range of values of sheet conductivity corresponding to the maximum values of attenuation. We feel that this difficulty

arises because in that range the attenuation is too large for the perturbation procedure we employ.

In addition to the foregoing the perturbation equation is applied in the determination of the initial slope of the phase velocity dispersion curve due to the mechanical effect of the thin film and excellent agreement is obtained with other[14] more direct approaches. Again, the iterative procedure is employed to obtain considerably more than the initial slope of the dispersion curve from the perturbation equation, and the results are shown to be extremely accurate. Finally, it should be noted that the perturbation theory is applicable in the determination of the attenuation due to all the aforementioned other causes. In particular, the attenuation resulting from the material viscosity of the substrate can readily be evaluated in the same manner using the results of Lamb and Richter[15] for quartz.

2. Piezoelectric Perturbation Theory

In this section we obtain a piezoelectric perturbation theory from a Green's function formulation[10] of linear piezoelectricity. To this end we write the equations of linear piezoelectricity in the form[16]

$$T_{ij,i} + T^{e}_{ij,i} = \rho \ddot{u}_j , \tag{2.1}$$

$$D_{i,i} + D^{e}_{i,i} = 0 , \tag{2.2}$$

$$T_{ij} = C^{E}_{ijk\ell} u_{k,\ell} + e_{kij} \varphi_{,k} ,$$

$$D_i = e_{ik\ell} u_{k,\ell} - \varepsilon^{S}_{ik} \varphi_{,k} , \tag{2.3}$$

where (2.1) and (2.2) are the stress equations of motion and charge equation of electrostatics, respectively; and (2.3) are the linear piezoelectric constitutive equations and T_{ij}, u_j and D_i denote the components of stress, mechanical displacement and electric displacement, respectively; ρ and φ denote

the mass density and electric potential, respectively; $c^{E}_{ijk\ell}$, e_{kij} and ϵ^{S}_{ij} denote the elastic, piezoelectric and dielectric constants, respectively. The quantities T^{e}_{ij} and D^{e}_{i} denote volumetric mechanical and electrical perturbation terms, respectively. In (2.1) - (2.3) we have employed the convention that a comma followed by an index denotes partial differentiation with respect to a space coordinate, the dot notation for differentiation with respect to time and the summation convention for repeated tensor indices.

The equations for the Green's tensor[17] corresponding to (2.1) - (2.3) may be written in the form

$$T^{\alpha}_{ij,i} + \rho\omega^2 G^{\alpha}_{j} = -\delta(P-Q)\delta^{\alpha}_{j}, \tag{2.4}$$

$$\mathcal{D}^{\alpha}_{i,i} = -\delta(P-Q)\delta^{\alpha}_{4}, \tag{2.5}$$

$$T^{\alpha}_{ij} = c^{E}_{ijk\ell} G^{\alpha}_{k,\ell} + e_{kij} f^{\alpha}_{,k},$$

$$\mathcal{D}^{\alpha}_{i} = e_{ik\ell} G^{\alpha}_{k,\ell} - \epsilon^{S}_{ik} f^{\alpha}_{,k}, \tag{2.6}$$

where α, $\beta = 1 - 4$, P and Q denote the fixed field point and variable source point, respectively, δ is the Dirac delta function, δ^{α}_{β} is the Kronecker delta, G^{α}_{j} and f^{α} are the mechanical displacement Green's tensor and electric potential Green's function plus cross terms, respectively, and the significance of the remaining quantities in (2.4) - (2.6) is obvious from (2.1) - (2.3). In (2.4) - (2.6) we have assumed that all variables have a time dependence of $e^{i\omega t}$. We now make the same assumption in (2.1) - (2.3) and in the usual manner, from (2.1) and (2.4), we form

$$\int_{V} \left[(T_{ij,i} + T^{e}_{ij,i} + \rho\omega^2 u_j) G^{m}_{j} - (T^{m}_{ij,i} + \rho\omega^2 G^{m}_{j} + \delta(P-Q)\delta^{m}_{j}) u_j \right] dV(Q) = 0, \tag{2.7}$$

where $m = 1 - 3$ and all variables in (2.7) have spatial dependence only. Employing the divergence theorem and using Eqs. (2.2), (2.3), (2.5) and (2.6), we obtain

$$u_m(P) = \int_S n_i\left[T_{ij}G_j^m - T_{ij}^m u_j + D_i f^m - \mathcal{B}_i^m\varphi\right] dS(Q) + \int_V \left[T_{ij,i}^e G_j^m + D_{i,i}^e f^m\right] dV(Q) . \tag{2.8}$$

Similarly, from (2.2) and (2.5) we form

$$\int_V \left[(D_{i,i} + D_{i,i}^e)f^4 - (D_{i,i}^4 + \delta(P-Q))\varphi\right] dV(Q) = 0 , \tag{2.9}$$

and utilizing the divergence theorem and (2.1), (2.3), (2.4) and (2.6), we obtain

$$\varphi(P) = \int_S n_i\left[D_i f^4 - \mathcal{B}_i^4\varphi + T_{ij}G_j^4 - T_{ij}^4 u_j\right] dS(Q) + \int_V \left[D_{i,i}^e f^4 + T_{ij,i}^e G_j^4\right] dV(Q) . \tag{2.10}$$

Equations (2.8) and (2.10) constitute the Green's function (or tensor) form of the equations of linear piezoelectricity. It turns out that in the sequel, although we have great use for (2.8) we have no use for (2.10) because of the particular type of perturbation problem of interest here.

Vibrational eigensolutions of the equations of linear piezoelectricity satisfy an equation which may be written in the form

$$\int_S n_i\left[T_{ij}^\mu u_j^\nu - T_{ij}^\nu u_j^\mu + D_i^\mu\varphi^\nu - D_i^\nu\varphi^\mu\right] dS = (\omega_\nu^2 - \omega_\mu^2)\int_V \rho u_j^\mu u_j^\nu \, dV , \tag{2.11}$$

where the scripts μ and ν refer to the μth and νth eigensolutions, respectively. It should be noted that (2.11) holds even if intermediate surfaces of discontinuity exist. Clearly, from (2.11), for homogeneous boundary conditions, we have

$$\int_V \rho u_j^\mu u_j^\nu \, dV = N_{(\mu)}^2 \delta_{\mu\nu} , \tag{2.12}$$

which is the orthogonality condition for piezoelectric vibrations. We now assume that a complete set of eigensolutions u_j^μ and φ^μ exists and define orthonormal eigensolutions to our eigenvibration or eigenwave problem by

$$g_j^\mu = u_j^\mu / N_{(\mu)} \ , \quad \hat{f}^\mu = \varphi^\mu / N_{(\mu)} \ . \tag{2.13}$$

We now expand the mechanical displacement Green's tensor G_j^m and electric potential Green's vector f^m in the forms

$$G_j^m = \sum_\mu M_\mu^m g_j^\mu \ , \quad f^m = \sum_\mu M_\mu^m \hat{f}^\mu \ , \tag{2.14}$$

where g_j^μ and $\hat{f}^\mu$ constitute orthonormal solution functions satisfying the appropriate homogeneous form of (2.1) - (2.3) subject to the appropriate boundary conditions. Substituting from (2.14) into (2.4), employing (2.6) and the homogeneous form of (2.4) for every μ, contracting with g_j^ν, integrating over V and utilizing (2.12), we obtain

$$M_\mu^m = g_m^\mu(P) / (\omega_\mu^2 - \omega^2) \ . \tag{2.15}$$

Substituting from (2.14) and (2.15) into (2.8), we obtain

$$u_m = \sum_\mu \frac{g_m^\mu(P)}{(\omega_\mu^2 - \omega^2)} \left[\int_S n_i [T_{ij} g_j^\mu(Q) - u_j T_{ij}^\mu(Q) + D_i \hat{f}^\mu(Q) - \varphi \mathcal{D}_i^\mu(Q)] \, dS(Q) \right.$$
$$\left. + \int_V [T_{ij,i}^e g_j^\mu(Q) + D_{i,i}^e \hat{f}^\mu(Q)] \, dV(Q) \right] . \tag{2.16}$$

We may now obtain our perturbation procedure from (2.16) in the usual way[9], i.e., by letting $u_m(P)$ be very near one of the g_j^μ, say g_m^1. Then we may write

$$u_m = g_m^1(P) + \sum_{\mu \neq 1} g_m^\mu(P) H_\mu / (\omega_\mu^2 - \omega^2) \ , \tag{2.17}$$

where

$$H_\mu = \int_S n_i \left[T_{ij} g_j^\mu - u_j T_{ij}^\mu + D_i \hat{f}^\mu - \varphi \mathcal{D}_i^\mu \right] dS + \int_V \left[T_{ij,i}^e g_j^\mu + D_{i,i}^e \hat{f}^\mu \right] dV \ , \tag{2.18}$$

and we have

$$H_1/(\omega_1^2 - \omega^2) = 1 , \tag{2.19}$$

which is the equation for the first perturbation in eigenfrequency. If

$$\Delta = \omega_1 - \omega , \tag{2.20}$$

from (2.19), we have

$$\Delta = H_1/2\omega_1 , \tag{2.21}$$

for the first perturbation in eigenfrequency. If we let the phase velocity v be written

$$v = v_1 - \epsilon , \tag{2.22}$$

then for constant wavenumber $\xi = \xi_1$, from (2.20) and (2.22), we have

$$\epsilon = \Delta/\xi_1 , \tag{2.23}$$

for the perturbation in phase velocity. Furthermore, if we let

$$\xi = \xi_1 + \delta , \tag{2.24}$$

then for constant $\omega = \omega_1$, from (2.22) - (2.24), we have

$$\delta = \Delta/v_1 , \tag{2.25}$$

for the perturbation in wavenumber.

We have discussed first order perturbation theory only because that is all we are interested in here. For a discussion of second and higher order perturbation theory see Ref.9.

Although the perturbation theory developed here is only for purely real perturbations of real eigenvalues, it may readily be formally generalized to the case of purely imaginary perturbations of <u>real</u> eigenvalues. This formal generalization is accomplished simply by requiring the T_{ij}, u_j, D_i and φ to be imaginary while the T^{μ}_{ij}, g^{μ}_j, D^{μ}_i and f^{μ} are real in Eq.(2.18). Then the H_{μ} in (2.18) is purely imaginary and the i is factored out before the integration is performed.

3. Attenuation Due to Air Loading

When the surface of the substrate is in contact with a fluid medium energy is transmitted from the acoustic surface wave to the fluid. Since the fluid has a much smaller mechanical impedance than the solid, the resulting attenuation can readily be calculated by finding the steady wave induced in the fluid by the small displacement at the surface of the substrate due to the known acoustic surface wave propagating along a free surface and employing (2.25) with (2.21) and (2.18). Since the fluid experiences small wave motion about a rest position, we may employ the linear equations for the small motion of a viscous, compressible fluid[19], which may be written in the form

$$\tau_{ij,i} = \rho_a \ddot{u}_j^a \,, \tag{3.1}$$

where

$$\tau_{ij} = \lambda^a u_{k,k}^a \delta_{ij} - \frac{2}{3}\mu^a \delta_{ij} \dot{u}_{k,k}^a + \mu^a (\dot{u}_{i,j}^a + \dot{u}_{j,i}^a) \,, \tag{3.2}$$

and λ^a, μ^a and ρ_a are the modulus of compression, coefficient of viscosity and mass density of the fluid, u_k^a denotes the components of the mechanical displacement vector of the fluid and δ_{ij} is the Kronecker delta.

A solution satisfying the differential equations and boundary conditions of linear piezoelectricity for acoustic surface waves[6,14,20,21] may be written in the form

$$u_j = \sum_{m=1}^{4} C^{(m)} A_j^{(m)} e^{i\beta_m \xi x_2} e^{i\xi(x_1 - \omega t)} \,,$$

$$\varphi = \sum_{m=1}^{4} C^{(m)} \bar{A}_4^{(m)} e^{i\beta_m \xi x_2} e^{i\xi(x_1 - \omega t)} \,, \tag{3.3}$$

for propagation in the direction x_1 with x_2 normal to the surface as shown in Fig.1. For a given set of boundary conditions, say traction-free and either short circuit or open circuit electrical conditions, values of $C^{(m)}$, $A_j^{(m)}$, $\bar{A}_4^{(m)}$ and β_m are determined numerically[6,14,20-22]. These calculations have been

performed for various cuts of lithium niobate[6,14,22] and quartz[20,23] including ST-cut quartz[22,24] and are assumed known for purposes of this work.

Since the amplitude of the mechanical displacement u_3 in the substrate is negligible compared to u_1 and u_2, we ignore u_3 in the treatment of the fluid and take the solution in the fluid in the form

$$u_1^a = \sum_{m=1}^{2} B^{(m)} D_1^{(m)} e^{\alpha_m \xi x_2} e^{i(\xi x_1 - \omega t)} ,$$

$$u_2^a = \sum_{m=1}^{2} B^{(m)} D_2^{(m)} e^{\alpha_m \xi x_2} e^{i(\xi x_1 - \omega t)} , \tag{3.4}$$

which satisfy (3.1), with (3.2), provided

$$i\omega\mu\left(\lambda - \frac{4}{3} i\omega\mu\right)\alpha_m^4 + \left[i\omega\mu\,(i\omega\mu + \rho_a V^2) + \left(\lambda - \frac{4}{3} i\omega\mu - \rho_a V^2\right)\left(\lambda - \frac{4}{3} i\omega\mu\right) - \left(\lambda - i\omega\frac{\mu}{3}\right)^2\right]\alpha_m^2 + \left[\lambda - \frac{4}{3} i\omega\mu - \rho_a V^2\right][i\omega\mu + \rho_a V^2] = 0 , \tag{3.5}$$

and

$$D_1^{(m)}/D_2^{(m)} = (\lambda - i\omega\mu/3)\, i\alpha_m/[\lambda - (4i\omega\mu/3) + i\omega\mu\,\alpha_m^2 - \rho_a V^2] , \tag{3.6}$$

where

$$V = \omega/\xi . \tag{3.7}$$

For a given ω and surface wave velocity V known from the aforementioned surface wave solutions[6,14,20-24] Eq. (3.5) is a biquadratic in α_m and yields four complex roots. The two corresponding to propagation away from the substrate in the x_2-direction are inserted in (3.4) and (3.6) for the solution. Moreover, these two solution functions decay with respect to distance from the surface of the substrate in the x_2-direction. The constants $B^{(m)}$ are determined from the values of u_1 and u_2 at the surface of the substrate, which is at $x_2 = 0$. For the solution in (3.4), the nontrivial components of the traction vector on planes normal to x_2 are given by

$$\tau_{21}^a = -\, i\omega\mu\,(u_{2,1}^a + u_{1,2}^a) ,$$

$$\tau_{22}^{a} = (\lambda + 2i\omega\mu/3)\, u_{1,1}^{a} + (\lambda - 4i\omega\mu/3)\, u_{2,2}^{(a)} \,. \tag{3.8}$$

In applying Eq. (2.18) and evaluating the normalization factor $N_{(\mu)}$ in (2.12) the integration is from the surface of the substrate at $x_2 = 0$ to infinity with respect to depth and over a wavelength of the acoustic surface wave. The normalized acoustic surface wave eigensolution is given by

$$g_j^1 = u_j/N_1 \,, \quad \hat{f}^1 = \varphi/N_1 \,, \tag{3.9}$$

where u_j and φ are given in (3.3), and from (2.12) and (3.3) we have

$$N_1^2 = i\,\frac{\pi}{\xi^2}\,\rho \sum_{m=1}^{4}\sum_{n=1}^{4} \frac{C^{(m)} A_k^{(m)} C^{(n)*} A_k^{(n)*}}{(\beta_m - \beta_n^*)} \,, \tag{3.10}$$

and * represents complex conjugate. The first perturbation of the eigenvalue may now be calculated from (2.18), which takes the form

$$H_1 = -\int_0^{2\pi/\xi} \Big[\tau_{21}^{a} g_1^1 + \tau_{22}^{a} g_2^1 \Big]_{x_2=0} dx_1 \,, \tag{3.11}$$

because $T_{2j} = 0$ at $x_2 = 0$ in the eigensolution in which the correct electrical continuity conditions have been employed so that the electrical terms in (2.18) cancel and the volumetric perturbation terms T_{ij}^{e} and D_i^{e} vanish identically in this problem. In accordance with the discussion at the end of Section 2, we now substitute the real part of (3.9) and the imaginary part of (3.8) into (3.11), factor out an i and perform the integration to obtain

$$H_1 = i\,\mathrm{Im}\Big[-\pi \sum_{m=1}^{2} \hat{B}^{(m)} \Big[(-i\omega\mu\, D_1^{(m)} \alpha_m + \omega\mu\, D_2^{(m)}) g_1^{*} + (i(\lambda + 2i\omega\mu/3)\, D_1^{(m)} + (\lambda - 4i\omega\mu/3)\, D_2^{(m)} \alpha_m) g_2^{*} \Big]_{x_2=0} \Big] \,, \tag{3.12}$$

where the $\hat{B}^{(m)}$ differ from the $B^{(m)}$ because of the normalization N_1 in the normalized surface wave solution which has been employed. The symbol Im denotes the imaginary part of the complex quantity in brackets in (3.12). Note that the real part of the complex quantity in brackets in (3.12) gives a small, relatively unimportant, change in surface wave velocity which we do not bother to present. The solution we have obtained can be improved by iterating in the manner discussed in the next two sections, but the present result is sufficiently accurate that it is not purposeful to iterate here.

When the viscosity μ of the fluid is neglected only the normal components of the mechanical displacement and traction force are continuous at the frictionless interface and in this case the solution reduces considerably. First, there is no sum in (3.4) because when $\mu = 0$ (3.5) yields only one root corresponding to a wave propagating away from the substrate. Then one need only eliminate the sum in (3.12) and set $\mu = 0$ wherever it occurs. Under these circumstances H_1 reduces to the considerably simpler form

$$H_1^r = i\pi\lambda(\omega^2/\xi^2)g_2 g_2^*/[(\omega^2/\xi^2) - (\lambda/\rho^a)]^{\frac{1}{2}} . \qquad (3.13)$$

Calculations have been performed for δ as a function of frequency using both (3.12) and (3.13) and the results are plotted in Fig.2. As can be seen from the figure, with increasing frequency there is increasing deviation. At a frequency of 1 GHz, the attenuation calculated from (3.12) is in very close agreement with the measurements of Szabo and Slobodnik[11] and, of course, the attenuation calculated from (3.13) is not. Bechmann's[25] constants for quartz were used in the calculation. The constants employed for the air at standard temperature and pressure (20°C and 1 atmosphere) are[26]

$$\rho_a = 1.21 \frac{Kg}{M^3} , \quad \lambda = 14.22 \times 10^4 \frac{N}{M^2} , \quad \mu = 18.22 \times 10^{-6} \frac{NS}{M^2} . \qquad (3.14)$$

Similar calculations have been performed for lithium niobate, and the results are plotted in Fig.3, which shows reasonable agreement with the measurements of Slobodnik[5].

4. Velocity Dispersion Due to Thin Films

When a thin film of a different material is plated on a substrate the fundamental essentially Rayleigh type surface wave becomes dispersive. Moreover, when the film is very thin compared with a wavelength, it has been shown[14,27] that approximate thin plate equations[28] can be used with great accuracy to treat the entire mechanical effect of the plating material as a boundary condition at the surface of the substrate. Both Skeie[29] and Auld[7] have used perturbation equations to calculate the initial slope of the Rayleigh wave dispersion curve due to a thin film. In this section we essentially repeat this calculation in order to emphasize the extreme accuracy with which the initial slope of the dispersion curve due to a thin surface film can be determined by means of perturbation theory. However, we go one step further and show how the equation for the first perturbation of the eigenvalue can be used iteratively to calculate with great accuracy considerably more than the initial slope.

The aforementioned approximate plate equations for a thin isotropic film plated on a substrate may be written in the form

$$T_{2j} = -\delta_{jb} 2h'\mu' \left[\left(\frac{3\lambda' + 2\mu'}{\lambda' + 2\mu'} \right) u_{a,ab} + u_{b,aa} \right] + 2h'\rho' \ddot{u}_j \ , \qquad (4.1)$$

where ρ', $2h'$ and λ', μ' are the mass density, thickness and Lamé constants, respectively, for the film material, the subscripts a and b can take the values 1 and 3 but not 2 and T_{2j} denotes the components of the traction vector at the surface of the substrate, which may be obtained from (2.3). In this application Eq. (2.18) takes the form

$$H_1 = - \int_0^{2\pi/\xi} \left[T_{2j} g_j^1 \right]_{x_2=0} dx_1 \ , \tag{4.2}$$

because the volumetric terms T_{ij}^e and D_i^e vanish identically, the boundary conditions employed in the surface wave solutions are $T_{2j}^1 = 0$ and $\hat{f}^1 = 0$ and $\varphi = 0$ in the conducting thin film. Substituting the real parts of (3.3) for the electrically shorted case and (4.1) into (4.2), taking the u_j in (4.1) to be the normalized u_j of the surface wave solution in (3.3) evaluated at the surface of the substrate and performing the integration, we obtain

$$H_1 = -\pi\gamma \left[\left(4\mu' \frac{(\lambda' + \mu')}{(\lambda' + 2\mu')} - \frac{\rho'\omega^2}{\xi^2} \right) g_1 g_1^* - \frac{\rho'\omega^2}{\xi^2} g_2 g_2^* + \left(\mu' - \frac{\rho'\omega^2}{\xi^2} \right) g_3 g_3^* \right], \tag{4.3}$$

where

$$\gamma = 2h'\xi \ , \tag{4.4}$$

and the g_j^1 are the components of the normalized displacement vector u_j at the interface. The initial slope of the phase velocity dispersion curve for an aluminum film on ST-cut quartz has been calculated from (4.3) and is plotted in Fig. 4 along with the correct curve. It is clear from the figure that the agreement of the initial slopes is excellent.

If the phase velocity determined from (4.3), with (2.21) - (2.23), for a small nonzero value of γ is inserted in the solution for ST-cut quartz[24,25], with the traction boundary conditions in (4.1) replacing the traction free conditions employed in the treatments, the system resulting from the differential equations may readily be solved for the four β_m and the accompanying amplitude ratios $A_j^{(m)}$ and then the system resulting from any two of the three traction boundary conditions along with the condition of vanishing potential may readily be solved for the amplitude ratios $C^{(1)} : C^{(2)} : C^{(3)} : C^{(4)}$. The resulting solution may then be employed in (2.18), which now takes the form

$$H_1 = - \int_0^{2\pi/\xi} \left[T_{2j} g_j^1 - T_{2j}^1 u_j \right]_{x_2=0} dX_1 , \tag{4.5}$$

to calculate a value of phase velocity at a nonzero value of γ. Equation (4.5) may then be used iteratively to calculate the phase velocity at a given value of γ to any desired degree of accuracy, subject only to the limitations inherent in (4.1). To this end we substitute the real parts of (3.3) for the electrically shorted case, (4.1) for T_{2j} and

$$T_{2j}^1 = c_{2jk\ell}^E g_{k,\ell}^1 + e_{k2j} f_{,k}^1 , \tag{4.6}$$

into (4.5), take u_j as before and perform the integration to obtain

$$H_1 = - \pi\gamma \left(\mu' - \rho' \frac{\omega^2}{\xi^2} \right) g_3^1 g_3^{1*} + \frac{\pi}{2\xi} \left(u_3 T_{23}^{1*} + u_3^* T_{23}^1 \right) , \tag{4.7}$$

where it has been assumed that the one boundary condition that has not been satisfied exactly is the condition on the traction T_{23}. For nonzero γ Eq. (4.7) may now be used iteratively to calculate the phase velocity to any desired degree of accuracy. The phase velocity dispersion curve for an aluminum film on ST-cut quartz has been calculated in this manner, and the resulting curve is indistinguishable from the correct curve shown in Fig.4. Similarly, the phase velocity dispersion curve for an aluminum film on Y-Z lithium niobate has been calculated and the results are plotted in Fig.5.

5. Attenuation Due to the Electrical Conductivity of Thin Films

When a thin conducting film is plated on the surface of a piezoelectric substrate carrying an acoustic surface wave, the attendant electric field causes currents to flow in the film. Since the film is thin compared with a wavelength, the full electrical conduction equations and associated boundary conditions need not be satisfied for the film and an approximate thin plate conductivity

equation can be obtained as noted in the Introduction. If we assume that the electric potential essentially does not vary across the thickness of the thin isotropic film and that the electric field E_i is derivable from the electric potential φ in the usual way, i.e., by

$$E_i = - \varphi_{,i} , \tag{5.1}$$

then application of the conservation of charge to the element of plate shown in Fig.6 yields

$$2h' \oint_C N_a J_a \, ds + \int_A \dot{D}_2 \, dS = 0 , \tag{5.2}$$

where N_a denotes the components of the unit normal in the plane and J_a denotes the components of the current in the plane. Substituting from Ohm's law

$$J_a = \sigma E_a , \tag{5.3}$$

(5.1) and employing the divergence theorem in the plane, we obtain

$$-2h'\sigma\varphi_{,aa} + \dot{D}_2 = 0 , \tag{5.4}$$

where σ is the electrical conductivity and D_2 may be determined from $(2.3)_1$ and the surface wave solution functions in (3.3). Substituting from (3.3) into (5.4), we obtain

$$\varphi(0) = i\omega D_2(0)/2h'\sigma\xi^2 , \tag{5.5}$$

where the notation (0) means evaluated at $x_2 = 0$, and the quantity $2h'\sigma$ is called the sheet conductivity of the thin surface film.

Even though we can readily include the mechanical influence of the film by means of Eq. (4.1), in this section we ignore this mechanical effect for reasons of expediency. Under these circumstances Eq. (2.18) takes the form

$$H_1 = - \int_0^{2\pi/\xi} \left[D_2 \hat{f}^1 - \varphi \hat{\vartheta}_2^1 \right]_{x_2=0} dx_1 , \tag{5.6}$$

because the volumetric terms T_{ij}^e and D_i^e vanish identically and the mechanical terms have been ignored. At this point it should be noted that had the mechanical terms been included, Eq. (5.6) would have resulted anyway if the correct dispersive surface wave solution were employed because then (4.1) would be used for both T_{2j} and T_{2j}^1 in (2.18). However, we do not bother with this refinement here. For future use we note that the complex equation (5.5) yields the purely real and purely imaginary equations

$$\varphi(0) + \varphi^*(0) = \frac{i\omega}{2h'\sigma\xi^2} \left(D_2(0) - D_2^*(0) \right) , \tag{5.7}$$

$$\varphi(0) - \varphi^*(0) = \frac{i\omega}{2h'\sigma\xi^2} \left(D_2(0) + D_2^*(0) \right) , \tag{5.8}$$

which we will have occasion to use separately in the sequel.

Since we are interested in obtaining results over an extremely large range of values of sheet conductivity $2h'\sigma$, we must perturb from the short circuit solution for large values of sheet conductivity and the open circuit solution for small values of sheet conductivity. To this end we first perturb from the short circuit surface wave eigensolution, in which $\hat{f}^1 = 0$, and in accordance with the discussion at the end of Section 2, consider a purely imaginary H_1, in which case (5.6) takes the form

$$H_1 = \frac{1}{4} \int_0^{2\pi/\xi} (\varphi - \varphi^*) (\hat{\vartheta}_2^1 + \hat{\vartheta}_2^{1*}) \, dx_1 . \tag{5.9}$$

Substituting from (5.8) into (5.9) and performing the integration, we obtain

$$H_1 = (i\omega\pi/2h'\sigma\xi^3) \hat{\vartheta}_2^1(0) \hat{\vartheta}_2^{1*}(0) , \tag{5.10}$$

where

$$\hat{\mathcal{D}}_2^1 = e_{2k\ell} g^1_{k,\ell} - \epsilon^S_{2k} \hat{f}^1_{,k} \,. \tag{5.11}$$

The attenuation calculated from (5.10) at a frequency of 100 MHz for ST-cut quartz is plotted as the curve marked short-circuit in Fig.7. This curve is valid for extremely large values of sheet conductivity only, which happens to be the region of practical interest. For somewhat smaller values of sheet conductivity, a considerably more accurate value of attenuation may be obtained in the following manner. First the corrected eigenvalue, including the determined time attenuation as well as the phase velocity, may be substituted in the system resulting from the solution of the piezoelectric differential equations, which may then readily be solved for the four β_m and the accompanying amplitude ratios $A_j^{(m)}$. Then the linear algebraic equations resulting from the three traction boundary conditions may be solved for the amplitude ratios $C^{(1)}:C^{(2)}:C^{(3)}:C^{(4)}$. The resulting solution may then be employed in (5.6), which for a purely imaginary H_1^I we take in the form

$$H_1^I = \frac{1}{4} \int_0^{2\pi/\xi} \left[(\varphi - \varphi^*)(\hat{\mathcal{D}}_2^1 + \hat{\mathcal{D}}_2^{1*}) - (D_2^* - D_2)(\hat{f}^1 + \hat{f}^{1*}) \right] dx_1 \,, \tag{5.12}$$

in order that the iterative perturbation procedure tend to satisfy the boundary condition (5.5), i.e., in order that H_1^I vanish for the exact solution that satisfies (5.5). For a purely real H_1^R, (5.6) takes the form

$$H_1^R = \frac{1}{4} \int_0^{2\pi/\xi} \left[(\varphi + \varphi^*)(\hat{\mathcal{D}}_2^1 + \hat{\mathcal{D}}_2^{1*}) - (D_2 + D_2^*)(\hat{f}^1 + \hat{f}^{1*}) \right] dx_1 \,. \tag{5.13}$$

Substituting from (5.8) into (5.12) and (5.7) into (5.13) and performing the integrations, we obtain

$$H_1^I = \frac{i\omega\pi}{2h'\sigma\xi^3}\,\hat{\mathcal{D}}_2^1\hat{\mathcal{D}}_2^{1*} - \frac{\pi}{2\xi}\,(\hat{f}^1 D_2^* - D_2\hat{f}^{1*}) \,, \tag{5.14}$$

$$H_1^R = -\frac{\pi}{2\xi}\,(\hat{f}^1 D_2^* + D_2\hat{f}^{1*}) \,, \tag{5.15}$$

where D_2 is to be taken to be the same as $\hat{\mathcal{D}}_2^1$ given in (5.11). Equation (5.14) determines the change in attenuation from any given state and Eq. (5.15) determines the change in phase velocity or frequency from any given state. Equations (5.14) and (5.15) may now be used iteratively to calculate the attenuation and phase velocity to any desired degree of accuracy as long as the attenuation is not too large. The attenuation calculated in the foregoing manner at a frequency of 100 MHz for ST-cut quartz yields the curve below the short-circuit curve in Fig. 7. The iterated attenuation calculation does not converge for values of sheet conductivity lower than the value at which the solid curve ends. We believe that this difficulty arises because the perturbation procedure we employ is for perturbations off real eigenvalues only, and in the region in which we cannot perform the calculation the attenuation is too large for the eigenvalue to be treated as approximately real for the accuracy required.

We now perturb from the open-circuit surface wave eigensolution, in which

$$\hat{\mathcal{D}}_2^1 = \epsilon_o \xi \hat{f}^1 \,, \tag{5.16}$$

by considering a purely imaginary H_1 in (5.6) which, with (5.16) takes the form

$$H_1 = \frac{1}{4}\int_0^{2\pi/\xi} \left[\epsilon_o \xi\,(\varphi - \varphi^*) - (D_2 - D_2^*)\right]\left[\hat{f}^1 + \hat{f}^{1*}\right] dx_1 \,. \tag{5.17}$$

Substituting from (5.7) into (5.17), taking φ to be $\hat{f}^1$ and performing the integration, we obtain

$$H_1 = (i\xi\pi 2h'\sigma/\omega)\hat{f}^1(0)\hat{f}^{1*}(0) \,. \tag{5.18}$$

The attenuation calculated from (5.18) at a frequency of 100 MHz for ST-cut quartz is plotted as the curve marked open-circuit in Fig.7. This curve is valid for relatively small values of sheet conductivity only. For somewhat larger values of sheet conductivity, a more accurate value of attenuation is obtained by using the corrected eigenvalue in the governing equations in the manner set forth in the short-circuit case and employing the resulting solution in (5.12) and (5.13), respectively, while substituting from (5.7) into (5.12) and (5.8) into (5.13) and performing the integrations to obtain

$$H_1^I = \frac{2h'\sigma i\pi\xi}{\omega} \hat{f}^1\hat{f}^{1*} + \frac{\pi}{2\xi} (\varphi\hat{\vartheta}_2^{1*} - \varphi^*\hat{\vartheta}_2^1), \tag{5.19}$$

$$H_1^R = \frac{\pi}{2\xi} (\varphi\hat{\vartheta}_2^{1*} + \varphi^*\hat{\vartheta}_2^1) . \tag{5.20}$$

Equations (5.19) and (5.20) may now be used iteratively to calculate the attenuation and phase velocity, respectively, to any desired degree of accuracy as long as the attenuation is not too large. The attenuation calculated in the foregoing manner at a frequency of 100 MHz for ST-cut quartz yields the curve below the open-circuit curve in Fig.7. This time the iterated attenuation calculation does not converge for values of sheet conductivity higher than the value at which the solid curve ends, and the reasons for this are the same as those discussed earlier in the short-circuit case. Similar calculations have been performed for Y-Z lithium niobate and the results are plotted in Fig.8.

Acknowledgement

This work was supported in part by the Office of Naval Research under Contract No. N00014-76-C-0368.

REFERENCES

1. P.H. Carr, "The Generation and Propagation of Acoustic Surface Waves at Microwave Frequencies," IEEE Trans. Microwave Theory Tech., MTT-17, 845 (1969).

2. G. Cambon and M. Rouzeyre, "Attenuation of Dispersive Rayleigh Waves on Quartz," Electron. Lett., 5, 539 (1970).

3. A.J. Slobodnik, Jr., P.H. Carr and A.J. Budreau, "Microwave Frequency Acoustic Surface-Wave Loss Mechanisms on $LiNbO_3$," J. Appl. Phys., 41, 4380 (1970).

4. J. Pouliquen and G. Vaesken, "Effect of a Metallic Thin Film on the Propagation of Rayleigh Waves," J. Appl. Phys., 44, 1524 (1973).

5. A.J. Slobodnik, Jr., "Surface Acoustic Waves and SAW Materials," IEEE Proc., 64, 581 (1976).

6. J.J. Campbell and W.R. Jones, "Propagation of Surface Waves at the Boundary Between a Piezoelectric Crystal and a Fluid Medium," IEEE Trans. Sonics Ultrason., SU-17, 71 (1970).

7. B.A. Auld, Acoustic Fields and Waves in Solids, Vol.II (John Wiley, New York, 1973), Chap.12.

8. K.A. Ingebrigtsen, "Linear and Nonlinear Attenuation of Acoustic Surface Waves in a Piezoelectric Coated with a Semiconducting Film," J. Appl. Phys., 41, 454 (1970).

9. P.M. Morse and H. Feshbach, Methods of Theoretical Physics, Part II (McGraw-Hill, New York, 1953), Chap.9, Sec.9.1.

10. H.F. Tiersten, Linear Piezoelectric Plate Vibrations (Plenum, New York, 1969), Chap.5.

11. T.L. Szabo and A.J. Slobodnik, Jr., "The Effect of Diffraction on the Design of Acoustic Surface Wave Devices," IEEE Trans. Sonics Ultrason., SU-20, 240 (1973).

12. H.F. Tiersten, unpublished lecture notes (1966).

13. R. Adler, "Simple Theory of Acoustic Amplification," IEEE Trans. Sonics and Ultrason., SU-18, 115 (1971).

14. B.K. Sinha and H.F. Tiersten, "Elastic and Piezoelectric Surface Waves Guided by Thin Films, J. Appl. Phys., 44, 4831 (1973).

15. J. Lamb and J. Richter, "Anisotropic Acoustic Attenuation with New Measurements for Quartz at Room Temperatures," Proc. Royal Soc. A, 293, 479 (1966).

16. Ref.10, Eqs.(5.24) - (5.29).

17. Ref.9, Sec.13.1.

18. Ref.10, Chap.8, Sec.7.

19. L. Malvern, Introduction to the Mechanics of a Continuous Medium (Prentice-Hall, Englewood Cliffs, New Jersey, 1969), Sec.6.3.

20. G.A. Coquin and H.F. Tiersten, "An Analysis of the Excitation and Detection of Piezoelectric Surface Waves in Quartz by Means of Surface Electrodes," J. Acoust. Soc. Am., 41, 921 (1967).

21. J.J. Campbell and W.R. Jones, "A Method for Estimating Optimal Crystal Cuts and Propagation Directions for Excitation of Piezoelectric Surface Waves," IEEE Trans. Sonics Ultrason., SU-15, 209 (1968).

22. G.W. Farnell and E.L. Adler, "Elastic Wave Propagation in Thin Layers," in Physical Acoustics, Vol.9, W.P. Mason and R.N. Thurston Eds. (Academic, New York, 1972), pp.35-127.

23. D. Penunuri and K.M. Lakin, "Surface Acoustic Wave Velocities of Isotropic Metal Films on Selected Cuts of $Bi_{12}GeO_{20}$, Quartz, Al_2O_3 and $LiNbO_3$," IEEE Trans. Sonics Ultrason., SU-21, 293 (1974).

24. A.J. Slobodnik, Jr., E.D. Conway and R.T. Delmonico, "Microwave Acoustics Handbook," Vol.1A, Air Force Cambridge Research Laboratories, AFCRL-TR-73-0597, p.576 (1973).

25. R. Bechmann, "Elastic and Piezoelectric Constants of Alpha Quartz," Phys. Rev., 110, 1060 (1958).

26. CRC Handbook of Chemistry and Physics, R.C. Weast and S.M. Selby, Eds., The Chemical Rubber Co. (1967).

27. H.F. Tiersten, "Elastic Surface Waves Guided by Thin Films," J. Appl. Phys., 40, 770 (1969).

28. R.D. Mindlin, "High Frequency Vibrations of Plated Crystal Plates," in Progress in Applied Mechanics (Macmillan, New York, 1963), pp.73-84.

29. H. Skeie, "Electrical and Mechanical Loading of a Piezoelectric Surface Supporting Surface Waves," J. Acoust. Soc. Am., 48, 1098 (1970).

FIGURE CAPTIONS

Figure 1 — Diagram Showing the Free Surface of a Semi-infinite Solid

Figure 2 — Attenuation of Surface Waves on ST-Cut Quartz due to Air Loading at Standard Temperature and Pressure (a) with and (b) without Fluid Viscosity. The dot is the value measured by Szabo and Slobodnik[11].

Figure 3 — Attenuation of Surface Waves on Y-Z Lithium Niobate due to Air Loading at Standard Temperature and Pressure (a) with and (b) without Fluid Viscosity. The dot is the value measured by Slobodnik[5].

Figure 4 — Lowest Straight-Crested Phase Velocity Dispersion Curve for an Aluminum Film on ST-Cut Quartz

Figure 5 — Lowest Straight-Crested Phase Velocity Dispersion Curve for an Aluminum Film on Y-Z Lithium Niobate

Figure 6 — Diagram Showing an Arbitrary Element of the Thin Conducting Film

Figure 7 — Attenuation of Surface Waves on ST-Cut Quartz due to Thin Conducting Films as a Function of Sheet Conductivity at a Frequency of 100 MHz

Figure 8 — Attenuation of Surface Waves on Y-Z Lithium Niobate due to Thin Conducting Films as a Function of Sheet Conductivity at a Frequency of 100 MHz

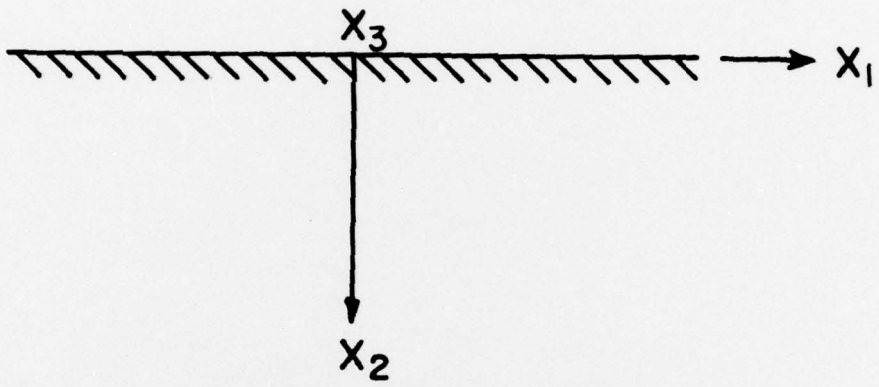

Figure 1

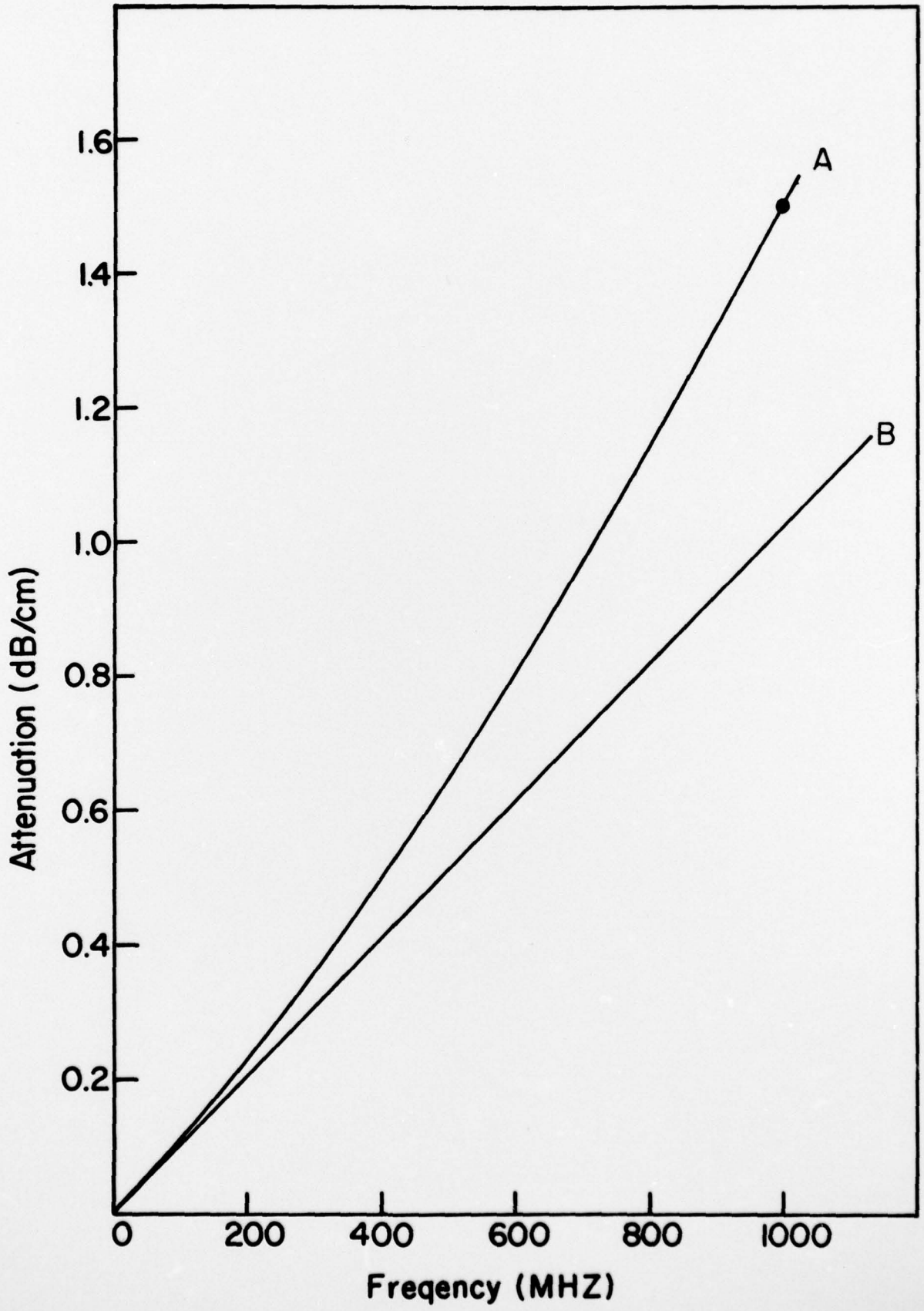
1.6
1.4
1.2
1.0
0.8
0.6
0.4
0.2
Attenuation (dB/cm)
A
B
0
200
400
600
800
1000
Freqency (MHZ)

Figure 2

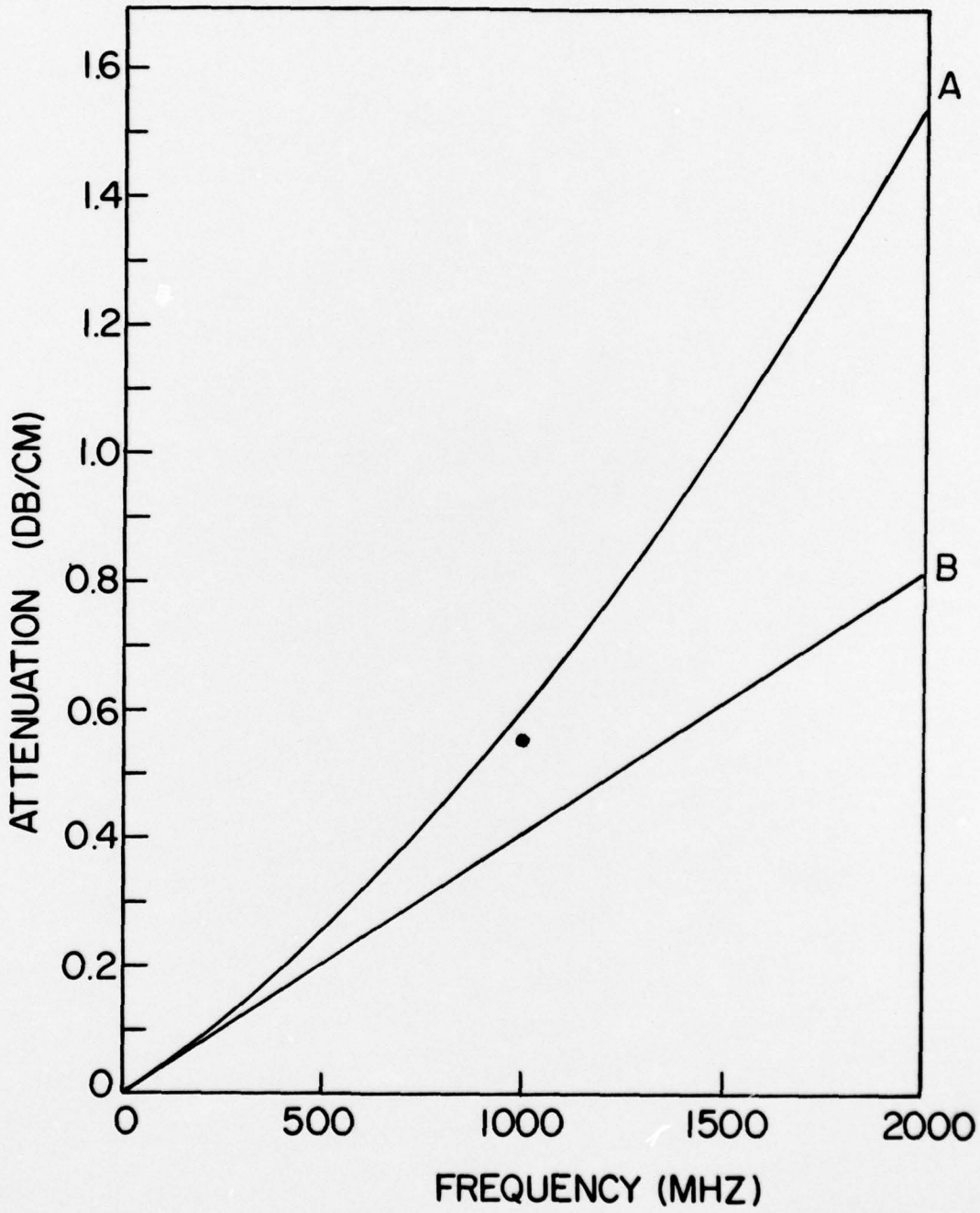
1.6
1.4
1.2
1.0
0.8
0.6
0.4
0.2
0
ATTENUATION (DB/CM)
A
B
0
500
1000
1500
2000
FREQUENCY (MHZ)

Figure 3

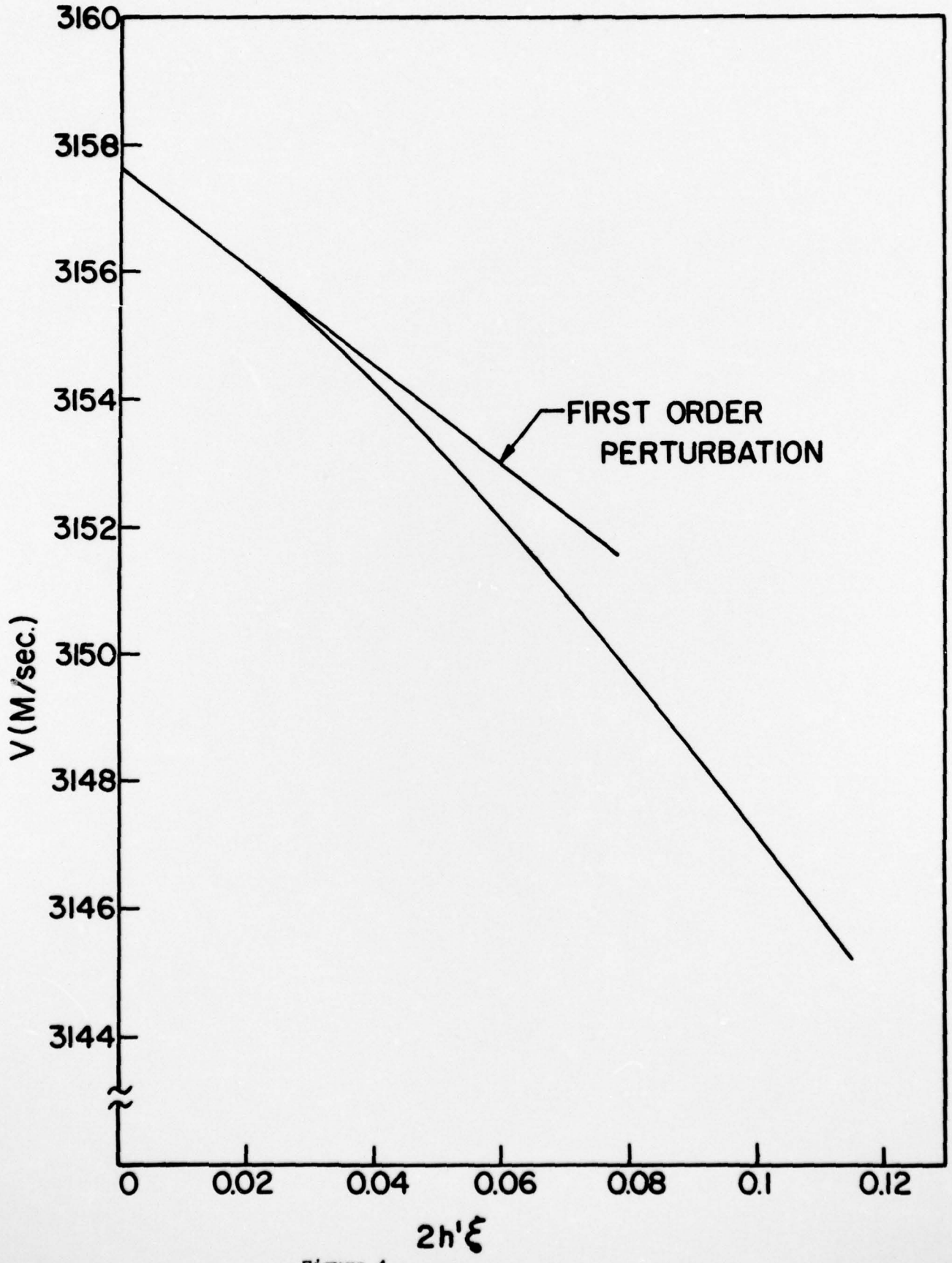
3160
3158
3156
3154
3152
3150
3148
3146
3144
V (M/sec.)
FIRST ORDER
PERTURBATION
0
0.02
0.04
0.06
0.08
0.1
0.12
2h'ξ

Figure 4

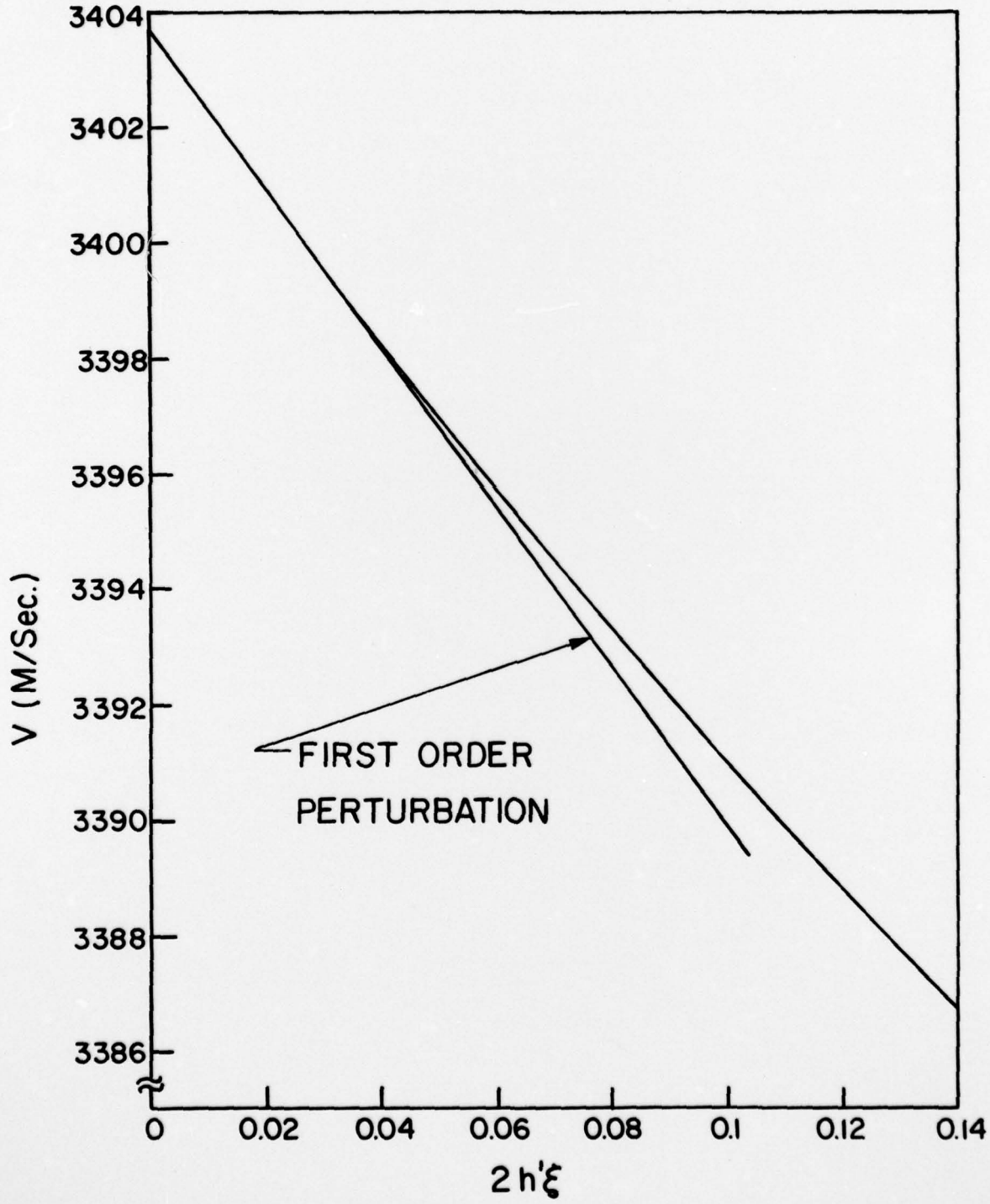
3404
3402
3400
3398
3396
3394
3392
3390
3388
3386
V (M/Sec.)
FIRST ORDER
PERTURBATION
0
0.02
0.04
0.06
0.08
0.1
0.12
0.14
2 h'ξ

Figure 5

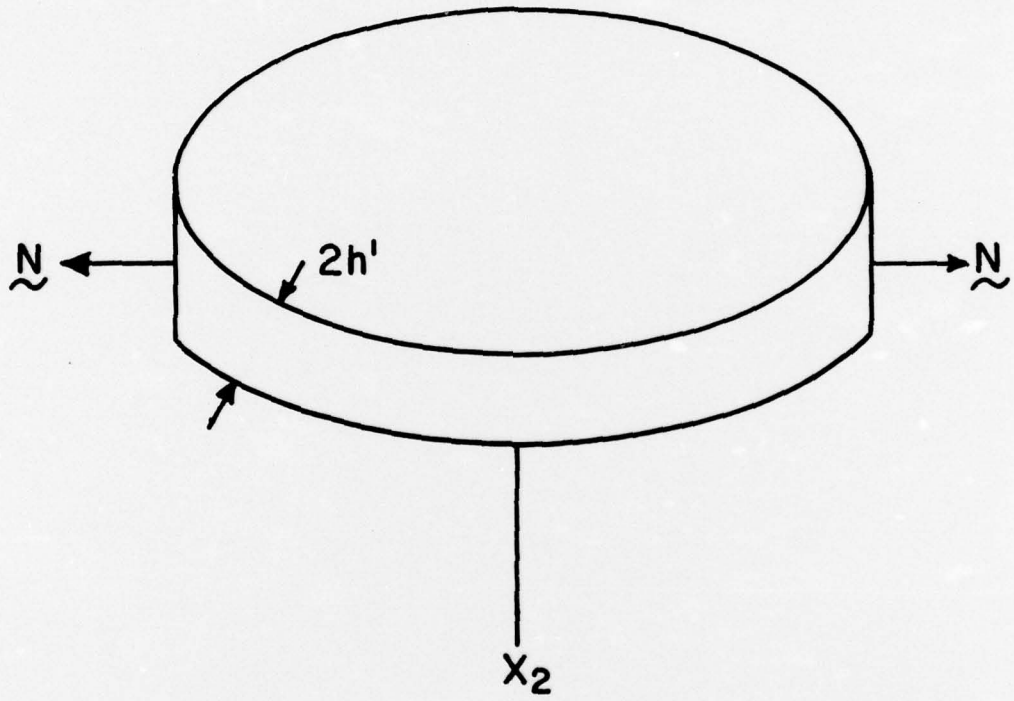

Figure 6

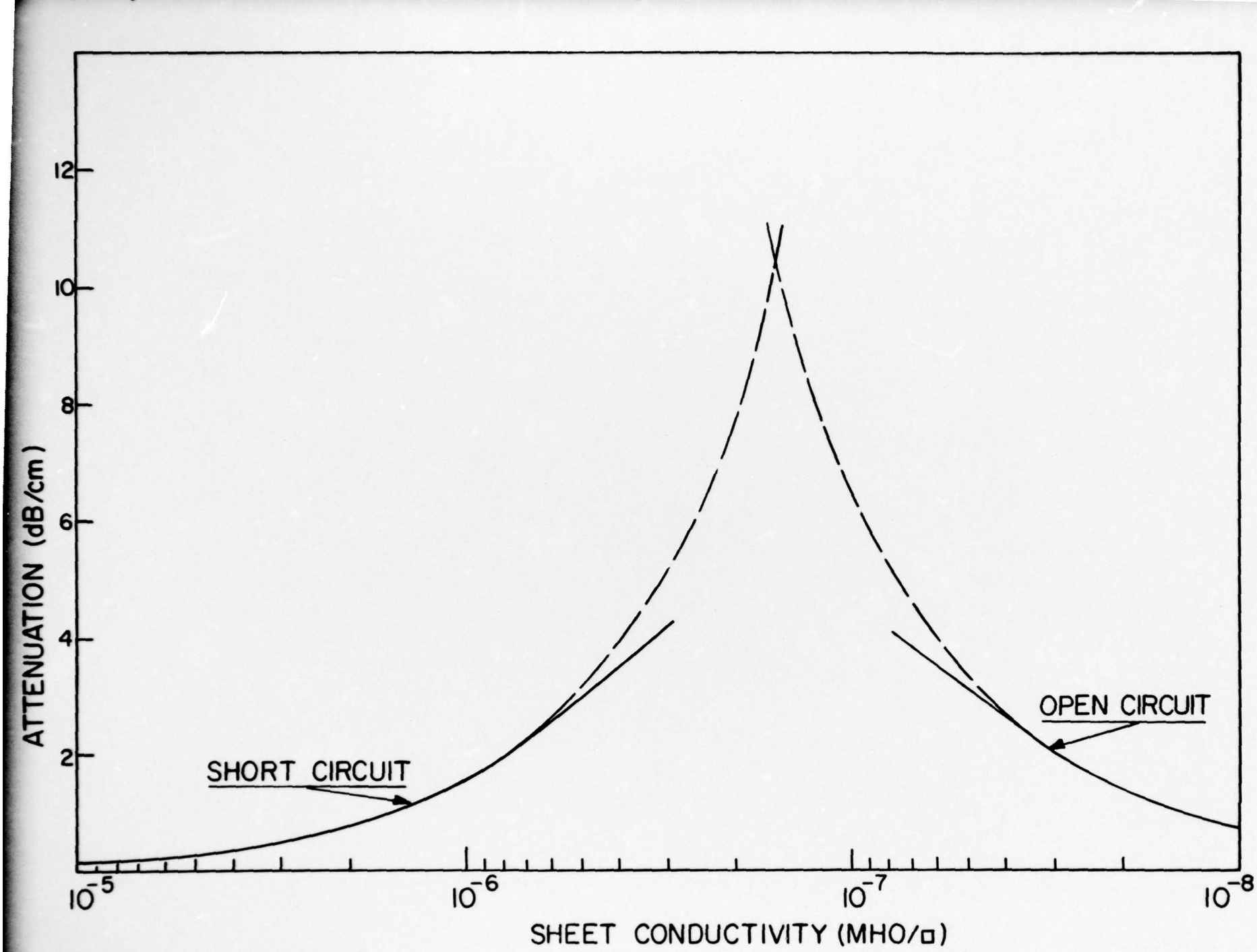
ATTENUATION (dB/cm)
12
10
8
6
4
2
SHORT CIRCUIT
OPEN CIRCUIT
10^{-5}
10^{-6}
10^{-7}
10^{-8}
SHEET CONDUCTIVITY (MHO/□)

Figure 7

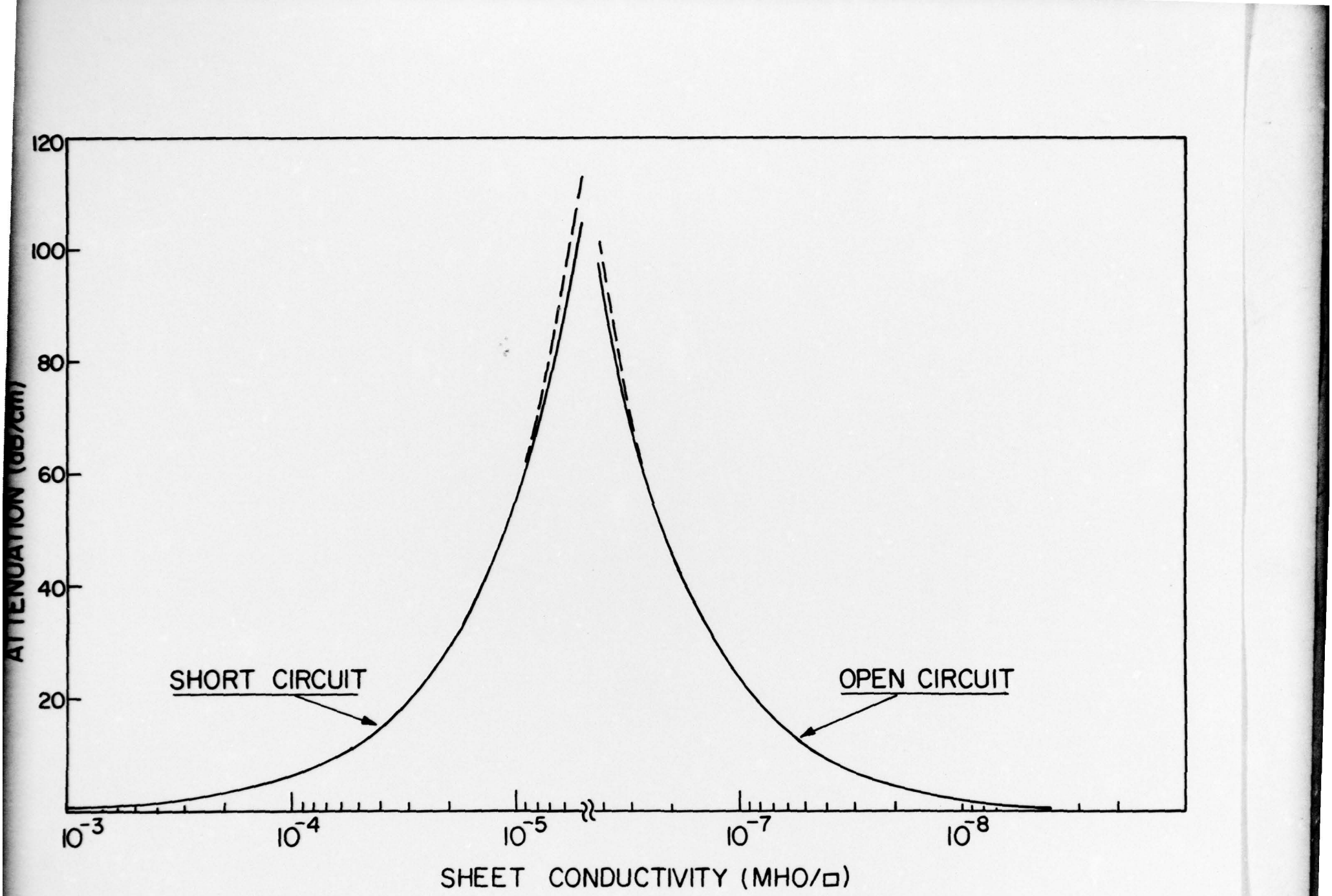
120
100
80
60
40
20
ATTENUATION (dB/cm)
SHORT CIRCUIT
OPEN CIRCUIT
10^{-3}
10^{-4}
10^{-5}
10^{-7}
10^{-8}
SHEET CONDUCTIVITY (MHO/□)

Figure 8